Analysis and Modeling of the Equilibrium Behaviors of U and Pu in Molten LiCI-KCI/Cd System at 500°C

Guy L. Fredrickson, Tae-Sic Yoo

September 2018



The INL is a U.S. Department of Energy National Laboratory operated by Battelle Energy Alliance

Analysis and Modeling of the Equilibrium Behaviors of U and Pu in Molten LiCI-KCI/Cd System at 500°C

Guy L. Fredrickson, Tae-Sic Yoo

September 2018

Idaho National Laboratory Idaho Falls, Idaho 83415

http://www.inl.gov

Prepared for the U.S. Department of Energy

Under DOE Idaho Operations Office Contract DE-AC07-05ID14517

Analysis and Modeling of the Equilibrium Behaviors of U and Pu in Molten LiCl-KCl/Cd System at 500°C

Guy L. Fredrickson and Tae-Sic Yoo Idaho National Laboratory, Pyroprocessing Department

Abstract

In the field of pyroprocessing of used nuclear fuels, liquid cadmium is applied in different ways to recover transuranics from molten salt, while effecting some degree of separations between transuranics and lanthanides. A model of the separation performance between uranium and plutonium across the phase boundary between molten salt and liquid cadmium is presented. The salt is the LiCl-KCl eutectic with solute concentrations of UCl₃ and PuCl₃. The cadmium is the liquid cadmium phase field from the Cd-U-Pu ternary alloy system. The model used to describe the behavior of uranium and plutonium in the salt/cadmium system is applied to describe the behavior of plutonium and lanthanide in the salt/cadmium system.

1. Introduction

The field of pyroprocessing includes a host of technologies that are applied to reprocessing used nuclear fuels. A primary goal of reprocessing in a closed fuel cycle is to keep the transuranics in the fuel cycle and out of the waste streams, while rejecting fission products from the fuel cycle and into the waste streams. The chemical interaction between molten salt and liquid metal is of great interest in this regard. The unique properties of cadmium are exploited to collect transuranics from molten salts while incurring some degree of separations between the transuranics and lanthanide fission products.

When such separations are performed by means of a cathodic potential to the cadmium, the technologies are often referred to as "liquid cadmium cathode" technologies. And when such separations are performed by means of chemical manipulations of the cadmium, the technologies are often referred to as "liquid metal extraction" technologies. The underlying principles involved with each family of technologies are very similar if not identical, particularly when the final condition is that of chemical equilibrium between the salt and cadmium phases. And the present investigation is concerned only with understanding the various states of this equilibrium.

Specifically, the molten salt is LiCl-KCl eutectic containing solute concentrations of UCl₃ and PuCl₃. The liquid cadmium contains dissolved uranium and plutonium up to the saturation limits of either metal. The temperature of interest is 500°C for reasons that will become apparent.

Experimentally derived phase diagrams for the Cd-U [1, 2], Cd-Pu [3], and U-Pu [4] binary alloy systems exist. However, an equivalent phase diagram for the Cd-U-Pu ternary alloy system does not exist. A conceptual phase diagram for the cadmium-rich end of the Cd-U-Pu system at 500°C is shown in Figure 1. At this temperature, cadmium forms a liquid phase with some solubility for uranium and plutonium. Uranium is dissolved in the liquid cadmium along the vertical axis; and uranium-saturated cadmium is in equilibrium with uranium metal. (At the slightly lower temperature of 473°C, the alloy system behaves differently and uranium-saturated cadmium is in equilibrium with intermetallic UCd₁₁.) Plutonium is dissolved in the liquid cadmium along the horizontal axis; and plutonium-saturated cadmium is in equilibrium with the plutonium-cadmium intermetallic PuCd₆. The slopes of the two phase boundaries between the "single" and "two phase" regions indicate that the saturation limit of uranium is decreased by the presence of plutonium; and likewise, the saturation limit of plutonium is decreased by the presence of uranium.

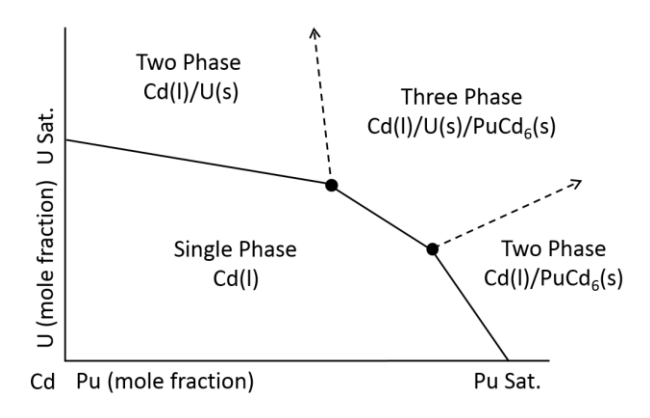


Figure 1. Conceptual Cadmium Phase Field at 500°C

A third phase boundary between the "single" and "three phase" regions though plausible, may or may not exist at 500°C. Upon considering i) the very small size of the liquid cadmium phase region in relation to the entirety of the complete Cd-U-Pu system, and ii) the lack of experimental information on the behavior of a potential three phase region, omission of the three phase region from further consideration appears justified because its presence, or lack thereof, does not significantly impact the forthcoming analysis. Allowing the omission of the three phase region, the phase boundaries between the single and two phase regions intersect as shown in Figure 2.

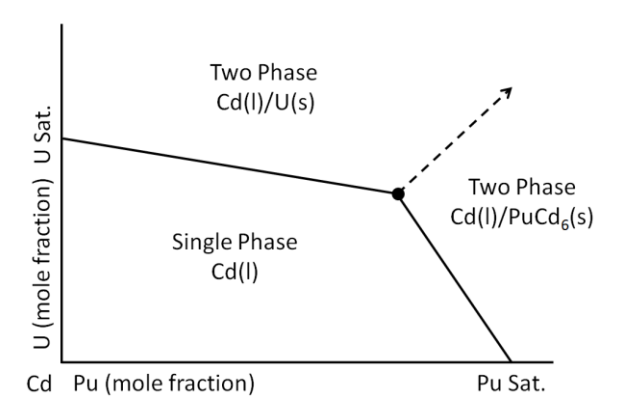


Figure 2. Simplified Cadmium Phase Field at 500°C

2. Phase Boundary Behavior

The solubility limits of uranium in cadmium [2] and of plutonium in cadmium [3] were previously measured over the temperature range of interest. The results from non-linear regression analyses (with SigmaStat Software [5]) of the original experimental data are expressed in Equations 1 and 2 for uranium

and Equations 3 and 4 for plutonium. These equations¹ give the solubility limits of uranium and plutonium in liquid cadmium as a function of temperature.

$$Log(mol\% U) = 5.65244 - \frac{3359.80}{T} - \frac{343095}{T^2} (for 321 to 472.4°C)$$
 (1)

$$Log(mol\% U) = 0.540417 - \frac{686.795}{T} + \frac{221289}{T^2} (for 472.4 to 650°C)$$
 (2)

$$Log(mol\% Pu) = 1.64901 - \frac{214.327}{T} - \frac{206062}{T^2} (for 355 to 406.8°C)$$
 (3)

$$Log(mol\% Pu) = 3.43269 - \frac{2211.27}{T} + \frac{311142}{T^2} (for 406.8 to 632°C)$$
 (4)

At 500°C, the solubility limits of uranium and plutonium in liquid cadmium are 1.127 and 1.798 mol. %, respectively; and the standard error of estimate for the two concentrations are 0.017 and 0.050 mol. %, respectively. Equations 1 through 4 are based on experimental data from binary alloy systems. Note that, as explained earlier, the uranium and plutonium behave differently in the Cd-U-Pu ternary system.

Figure 3 is a geometric interpretation of the phase diagram shown in Figure 2. The numeric values of the individual solubility limits of uranium and plutonium in cadmium at 500°C are labeled on the vertical and horizontal axes, respectively. The Cd/U and Cd/PuCd₆ phase boundaries are *assumed to be linear* and are represented by Equations 5 and 6, respectively. These two phase boundaries intersect at the inflection point denoted in Equation 7.

$$X_U = a_1 X_{Pu} + b_1 \tag{5}$$

$$X_{II} = a_2 X_{PII} + b_2 (6)$$

$$X_{Pu}^*, X_{II}^* \tag{7}$$

In these equations: subscript 1 applies to terms in the equation describing the Cd/U phase boundary; subscript 2 applies to terms in the equation describing the Cd/PuCd₆ phase boundary; X_U and X_{Pu} are the mole fractions of uranium and plutonium dissolved in the cadmium, respectively; a_i and b_i are slope and intercept constants. The mole fractions with an asterisk designate the composition of the inflection point. As an additional constraint, it is assumed that *the inflection point is restricted to lie along the diagonal line* shown in Figure 3. This diagonal line represents a constant U:Pu ratio during co-saturation based on the ratio of the individual saturation limits of uranium and plutonium in the binary alloy systems.

¹ More significant figures are presented here than are justified by the quality of the experimental data. Values of mol. % should be rounded to four significant figures if used in further calculations or three significant figures if the absolute values are sought. Temperature (*T*) is in units of degrees Celsius.

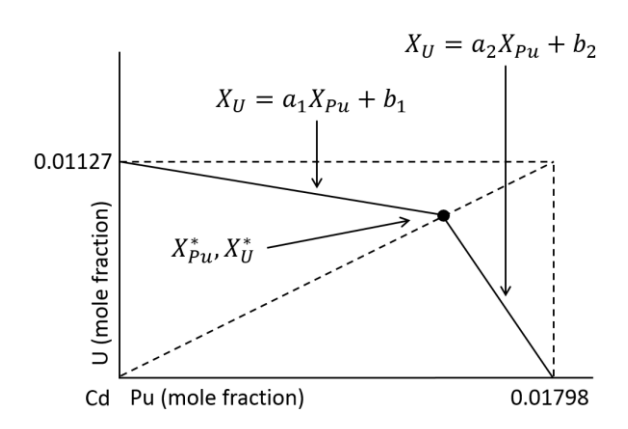


Figure 3. Geometric Interpretation of the Cadmium Phase Field at 500°C

In the systems of interest to pyroprocessing, the liquid cadmium is in contact with molten salt as described earlier and the resulting exchange reaction between these two phases is shown in Equation 8. The following analysis assumes *that thermodynamic equilibrium is achieved* between the UCl₃ and PuCl₃ dissolved in the salt, and the uranium and plutonium metals dissolved in the cadmium.

$$PuCl_3(salt) + U(cadmium) = UCl_3(salt) + Pu(cadmium)$$
 (8)

The following equations describe the thermodynamic equilibrium between the salt and cadmium phases as expressed in Equation 8.

$$\Delta G_{f,UCl_3}^0 - \Delta G_{f,PuCl_3}^0 = RT ln \left(\frac{a_{PuCl_3}}{a_{Pu}(a_{Cl_2})^{1.5}} \right) - RT ln \left(\frac{a_{UCl_3}}{a_{U}(a_{Cl_2})^{1.5}} \right)$$
(9)

$$\frac{\gamma_{U}X_{U}}{\gamma_{Pu}X_{Pu}} = exp\left(\frac{\Delta G_{f,UCl_{3}}^{0} - \Delta G_{f,PuCl_{3}}^{0}}{RT}\right) \frac{\gamma_{UCl_{3}}X_{UCl_{3}}}{\gamma_{PuCl_{3}}X_{PuCl_{3}}}$$
(10)

where,

 $\Delta G_{f,i}^0 = standard\ state\ Gibbs\ free\ energy\ of\ formation\ of\ species\ i$

 $a_i = chemical \ activity \ of \ species \ i$

 $\gamma_i = activity coefficent of species i$

 $X_i = mole \ fraction \ of \ species \ i$

 $R = universal\ gas\ constant$

T = temperature, K

For the present purpose of focusing on metal phase behavior, it is assumed that the activity coefficients of UCl₃ and PuCl₃ are constant over the concentration and temperature ranges of interest. Then, Equation 10 is simplified further.

$$\frac{\gamma_U X_U}{\gamma_{Pu} X_{Pu}} = k \frac{X_{UCl_3}}{X_{PuCl_3}} \tag{11}$$

$$k = exp\left(\frac{\Delta G_{f,UCl_3}^0 - \Delta G_{f,PuCl_3}^0}{RT}\right) \frac{\gamma_{UCl_3}}{\gamma_{PuCl_3}}$$
(12)

The thermodynamic data used to calculate k are given in Table 1. The "super cooled" liquid standard states for UCl₃ and PuCl₃ were used in the calculations of the standard state Gibbs free energy of formation.

The value of k is highly sensitive to the terms within the exponent. And the sensitivity of k is compounded by the exponent containing an expression for the relatively small difference between two relatively large measurement values (i.e., the two Gibbs free energy terms). Such mathematical realities explain, in part, the challenge of building high fidelity thermodynamic models. Thus, the selection of the thermodynamic data used to calculate k is certainly an important consideration. However, rather than focusing on deriving the most accurate value of k, it is more important at this time to simply appreciate that k is treated here as a constant.

•		•
Parameter	Value	Reference
$\Delta G_{f,UCl_3}^0$ at 500°C	-684.796 kJ mol ⁻¹	[6]
$\Delta G_{f,PuCl_3}^0$ at 500°C	-771.377 kJ mol ⁻¹	[6]
γ_{UCl_3}	0.00579	[7]
γ_{PuCl_3}	0.00662	[7]
R	8.31451 J K ⁻¹ mol ⁻¹	[8]
T	773.15 K	
K	6.182E5	

Table 1. Thermodynamic Values Used in Equation 12

Referring to the Cd/U phase diagram at 500°C [1], uranium saturated cadmium is in equilibrium with uranium metal (which, by definition, has unit activity of uranium). Then, the activity and activity coefficient of uranium in cadmium are described by Equations 13 and 14, respectively.

$$a_{U} = 1 = \gamma_{U} X_{U} = \gamma_{U} 0.01127 \tag{13}$$

$$\gamma_U = \frac{1}{0.01127} = 88.72 \tag{14}$$

The activity of uranium and the activity coefficient of plutonium are assumed to be invariant along the Cd/U phase boundary described by Equation 5 and as shown in Figure 3. These relationships are expressed as follows.

$$a_{U,1} = \gamma_{U,1} X_{U,1} = c_1 = 1 \tag{15}$$

$$\gamma_{Pu,1} = unknown constant$$
 (16)

Similarly, referring to the Cd/Pu phase diagram at 500°C [3], plutonium saturated cadmium is in equilibrium with the intermetallic PuCd₆ (which has less than unit activity of plutonium). Then, the activity and activity coefficient of plutonium in cadmium are described by Equations 17 and 18, respectively. The activity of plutonium is calculated from available experimental data [3].

$$a_{Pu} = 4.370E - 6 = \gamma_{Pu} X_{Pu} = \gamma_{Pu} 0.01798 \tag{17}$$

$$\gamma_{Pu} = \frac{4.370E - 6}{0.01798} = 2.431E - 4 \tag{18}$$

The activity of plutonium and the activity coefficient of uranium are assumed to be invariant along the Cd/PuCd₆ phase boundary described by Equation 6 and as shown in Figure 3. These relationships are expressed as follows.

$$a_{Pu,2} = \gamma_{Pu,2} X_{Pu,2} = c_2 = 4.370E-6 \tag{19}$$

$$\gamma_{U,2} = unknown \ constant$$
 (20)

Equation 16 reflects that the activity of plutonium is not constant along the Cd/U phase boundary and, likewise, Equation 20 reflects that the activity of uranium is not constant along the Cd/PuCd₆ phase boundary. However, there must be continuity of activities as the composition of the cadmium phase approaches the phase boundaries or the inflection point from any direction.

The inflection point represented by Equation 7 has a unique set of conditions. Adapting Equation 11 to represent the inflection point gives the following, where k has the same meaning and value as before.

$$\frac{\gamma_U^* X_U^*}{\gamma_{Pu}^* X_{Pu}^*} = k \frac{X_{UCl_3}^*}{X_{PuCl_2}^*} \tag{21}$$

The activity coefficient of uranium at the inflection point is equal to the activity coefficient of uranium along the Cd/PuCd₆ phase boundary.

$$\gamma_U^* = \gamma_{U,2} \tag{22}$$

Then, the activity of uranium along the Cd/PuCd₆ phase boundary is expressed as follows.

$$a_{U,2} = \gamma_{U,2} X_U = \gamma_U^* X_U \tag{23}$$

Also, the activity of uranium at the inflection point is equal to the activity of uranium along the Cd/U phase boundary.

$$\gamma_U^* X_U^* = \gamma_{U,1} X_{U,1} = c_1 = 1 \tag{24}$$

The activity coefficient of plutonium at the inflection point is equal to the activity coefficient of plutonium along the Cd/U phase boundary.

$$\gamma_{Pu}^* = \gamma_{Pu.1} \tag{25}$$

Then, the activity of plutonium along the Cd/U phase boundary is expressed as follows.

$$a_{Pu,1} = \gamma_{Pu,1} X_{Pu} = \gamma_{Pu}^* X_{Pu} \tag{26}$$

Finally, the activity of plutonium at the inflection point is equal to the activity of plutonium along the Cd/PuCd₆ phase boundary.

$$\gamma_{Pu}^* X_{Pu}^* = \gamma_{Pu,2} X_{Pu,2} = c_2 = 4.370E-6 \tag{27}$$

Equations 21, 24 and 27 are combined to give the following Pu:U molar ratio in the salt at the inflection point.

$$\frac{X_{PuCl_3}^*}{X_{UCl_3}^*} = 2.702 \tag{28}$$

Equation 24 is rearranged to give the activity coefficient of uranium in cadmium at the inflection point.

$$\gamma_U^* = \frac{1}{X_U^*} \tag{29}$$

Equation 27 is rearranged to give the activity coefficient of plutonium in cadmium at the inflection point.

$$\gamma_{Pu}^* = \frac{4.370E - 6}{X_{Pu}^*} \tag{30}$$

Identifying the location of the inflection point will lead to numeric solutions of Equations 29 and 30.

3. Inflection Point Identification

Figure 3 is redrawn as Figure 4 to include experimental data from the literature [9, 10] that are representative of the composition of the cadmium phase under various conditions of co-saturation of uranium and plutonium. Direct extraction (DE) and electrochemical extraction (EE) describe two different approaches of equilibrating the salt and cadmium phases [10]. Within experimental error, these data fall along the Cd/U and Cd/PuCd₆ phase boundaries.

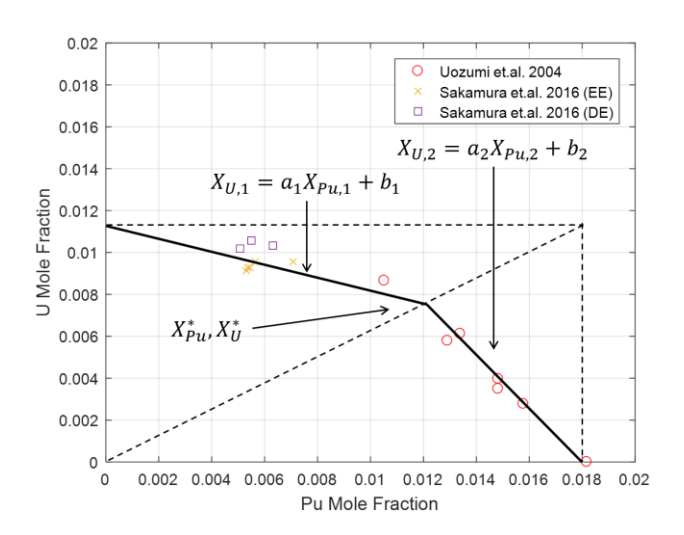


Figure 4. Geometric Interpretation of the Cadmium Phase Field at 500°C with Experimental Data

The solution strategy used to determine the inflection point relies on the minimization of the sum of squared errors, via nonlinear least squares regression analysis, of two linear equations. The constraint is that the inflection point (a.k.a., point of intersection) lies along the diagonal established by the independent saturation limits of uranium and plutonium in cadmium.

The mechanics of the solution strategy are briefly described. Equations 31 and 32 are the linear equations that describe the Cd/U and Cd/PuCd₆ phase boundaries, respectively.

$$y = f_1(x, x^*) = a_1(x^*)x + b_1 \tag{31}$$

$$y = f_2(x, x^*) = a_2(x^*)x + b_2(x^*)$$
(32)

Equation 33 describes the set of experimental data.

$$D = \{(x_i, y_i) | i = 1, ..., n\}$$
(33)

Equations 34 and 35 describe the partitioning of experimental data along the Cd/U and Cd/PuCd₆ phase boundaries, respectively.

$$I_1 = \{j \mid (x_j, y_j) \in D \land y_j X_{Pu,sat} > x_j X_{U,sat}\}$$
(34)

$$I_2 = \{k | (x_k, y_k) \in D \land y_k X_{Pu,sat} \le x_k X_{U,sat}\}$$

$$(35)$$

Equations 36 and 37 describe the error in terms of the difference between the experimental data and the derived linear Cd/U and Cd/PuCd₆ phase boundaries, respectively.

$$r_j = y_j - f_1(x_j, x^*), j \in I_1$$
 (36)

$$r_k = y_k - f_2(x_k, x^*), k \in I_2$$
 (37)

Equation 38 describes the solution criteria of the argument that minimizes the sum of squared errors and the Pu:U ratio constraint along the diagonal.

$$X_{Pu}^* = \arg\min_{x^*} \left(\sum_j r_j^2 + \sum_k r_k^2 \right); \ X_U^* = \frac{0.01127}{0.01798} X_{Pu}^*$$
 (38)

The inflection point identified by Equation 38 and the parameters derived for the Cd/U and Cd/PuCd₆ phase boundaries are given in Equations 39 to 41.

$$a_1 = -0.3077; b_1 = 0.01127$$
 (39)

$$a_2 = -1.2769; b_2 = 0.02296$$
 (40)

$$X_U^* = 0.007559; X_{Pu}^* = 0.01206$$
 (41)

The composition at the inflection point is used to calculate the activity coefficients of uranium and plutonium at the inflection point.

$$\gamma_U^* = \frac{1}{X_U^*} = 132.29 \tag{42}$$

$$\gamma_{Pu}^* = \frac{4.370E-6}{X_{Pu}^*} = 3.6237E-4 \tag{43}$$

The results thus far describing the thermodynamic behavior of the liquid cadmium phase field in the Cd-U-Pu phase diagram shown in Figure 4 are summarized in Table 2.

Table 2. Thermodynamic Values Derived from Solution Strategy

Parameter	Value
Saturation limit of U in Cd-U binary alloy.	0.01127 mole fraction
Activity coefficient of U in Cd-U binary alloy.	88.73
Saturation limit of Pu in Cd-Pu binary alloy.	0.01798 mole fraction
Activity coefficient of Pu in Cd-Pu binary alloy.	2.4310E-4
Equation describing the Cd/U phase boundary.	$X_{U,1} = -0.3077 X_{Pu,1} + 0.01127,$ or $X_{Pu,1} = -3.2499 X_{U,1} + 0.03663$
Equation describing the Cd/PuCd ₆ phase boundary	$X_{U,2} = -1.2769 X_{Pu,2} + 0.02296,$ or $X_{Pu,2} = -0.7831 X_{U,2} + 0.01798$
Location of Inflection Point	$X_U^* = 0.007559$ $X_{Pu}^* = 0.01206$
Activity of U along the Cd/U phase boundary.	1
Activity coefficient of U along the Cd/PuCd ₆ phase boundary.	132.29
Activity of Pu along the Cd/PuCd ₆ phase boundary.	4.370E-6
Activity coefficient of Pu along the Cd/U phase boundary.	3.6237E-4

4. Separation Factors along the Phase Boundaries

Separation factor (SF) is defined here as a ratio of two ratios; the Pu:U ratio in the salt divided by the Pu:U ratio in the cadmium.

$$SF = \frac{(X_{PuCl_3}: X_{UCl_3})_{Salt}}{(X_{Pu}: X_U)_{Cadmium}} = \frac{X_{PuCl_3} X_U}{X_{UCl_3} X_{Pu}}$$
(44)

From Equation 28, a Pu:U ratio in the salt less than 2.702 exist along the Cd/U phase boundary, and a Pu:U ratio in the salt greater than 2.702 exist along the Cd/PuCd₆ phase boundary.

The specific chemical interaction between the salt and cadmium phases introduced in Equation 8, represents the equilibrium with respect to UCl₃ and PuCl₃ dissolved in the salt and uranium and plutonium dissolved in the cadmium. The equilibrium concentrations of these four solute species are interdependent of each other according to well established thermodynamic principles.

The mechanics for describing the composition of the cadmium phase along the Cd/U and Cd/PuCd₆ phase boundaries are completely described in the preceding analyses. Correspondingly, similar mechanics are used to describe the compositions of the salt phase and, consequently, the resultant separation factors along the two phase boundaries.

Algebraic manipulations of Equations 5, 11, 24, and 44 give Equation 45, which describes the separation factor along the Cd/U phase boundary.

$$SF_1 = \frac{X_{PuCl_3}X_{U,1}}{X_{UCl_3}X_{Pu,1}} = \frac{X_{PuCl_3}}{X_{UCl_3}}a_1 + k\gamma_{Pu,1}b_1, \text{ for } 0 < \frac{X_{PuCl_3}}{X_{UCl_3}} < 2.702$$
 (45)

The separation factor has a limiting value as the Pu:U ratio in the salt approaches zero.

$$\lim_{X_{PuCl_3}/X_{UCl_3} \to 0} SF_1 = k\gamma_{Pu,1}b_1 = 2.525 \tag{46}$$

Similar algebraic manipulations of Equations 6, 11, 27, and 44 give Equation 47, which describes the separation factor along the Cd/PuCd₆ phase boundary.

$$SF_2 = \frac{X_{PuCl_3} X_{U,2}}{X_{UCl_3} X_{Pu,2}} = \left(\frac{X_{UCl_3}}{a_2 X_{PuCl_3}} - \frac{\gamma_{U,2} b_2}{k a_2 c_2}\right)^{-1}, \text{ for } \frac{X_{PuCl_3}}{X_{UCl_3}} \ge 2.702 \tag{47}$$

The separation factor has a limiting value as the Pu:U ratio in the salt approaches infinity.

$$\lim_{X_{PuCl_3}/X_{UCl_3} \to \infty} SF_2 = -\frac{ka_2c_2}{\gamma_{U,2}b_2} = 1.136$$
 (48)

The separation factor as a function of the Pu:U ratio in the salt, for conditions unique to the Cd/U and Cd/PuCd₆ phase boundaries is shown in Figure 5 with experimental data from the literature [10] that are representative of the composition of the cadmium phase under various conditions of co-saturation of uranium and plutonium. The dashed lines represent the upper and lower separation factor limits according to Equations 46 and 48, respectively. These limits provide the theoretical separation performance bounds of the system under equilibrium conditions.

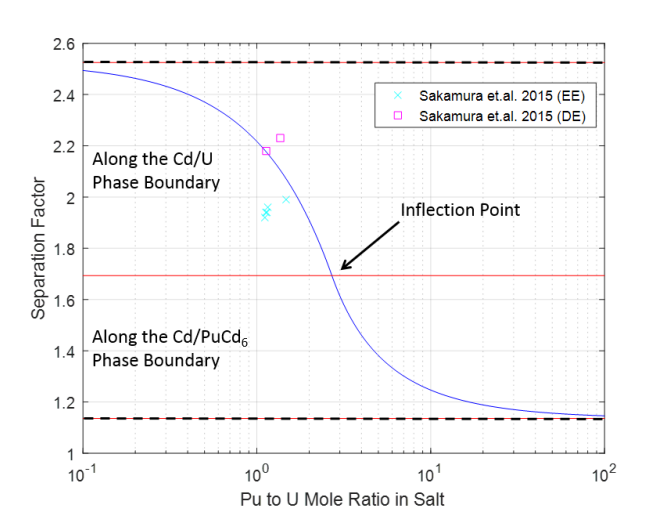


Figure 5. Conditions along the Phase Boundaries

Equations 28, 41, and 44 are combined to give the separation factor at the inflection point.

$$SF^* = \frac{X_{PuCl_3}^* X_U^*}{X_{UCl_3}^* X_{Pu}^*} = 2.702 \frac{0.007559}{0.01206} = 1.694$$
 (49)

5. Undersaturated Behavior

A geometric interpretation of a condition, N, within the cadmium phase field is shown in Figures 6A and 6B. The segment AB is the Cd/U phase boundary. Likewise, the segment CB is the Cd/PuCd $_6$ phase boundary.

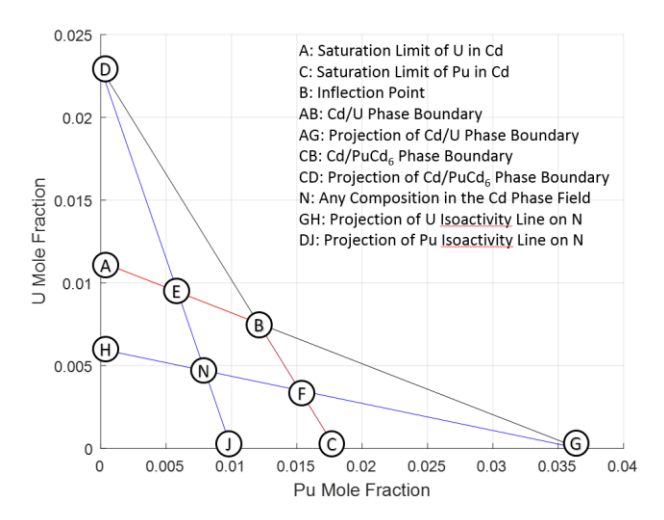


Figure 6A. Geometric Interpretation of Conditions within the Phase Boundaries

Lines AG and CD are fixed and defined by Equations 5 and 6, respectively. Lines HG and JD are variable and allowed to pivot at points G and D, respectively, in response to the position of point N. At any point N, (x_N, y_N) , within the cadmium phase field, the corresponding points E, (x_1, y_1) , and F, (x_2, y_2) , are readily determined by solving for the intersections of known lines.

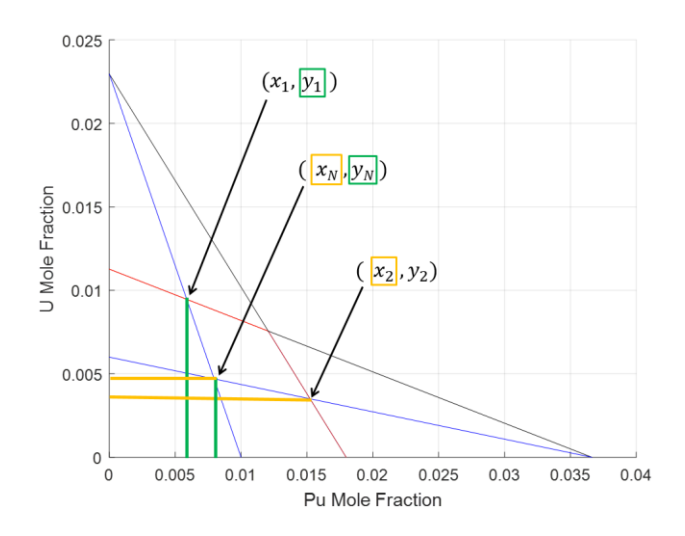


Figure 6B. Geometric Interpretation of Conditions within the Phase Boundaries

The preceding geometric interpretation leads to the following undersaturated domain model for the activities of uranium and plutonium in cadmium at point N.

$$a_{U,N} = \gamma_{U,N} X_{U,N} = a_{U,AG} \frac{y_N}{y_1} = \frac{X_{U,N}}{y_1}$$
(50)

$$a_{Pu,N} = \gamma_{Pu,N} X_{Pu,N} = a_{Pu,CD} \frac{x_N}{x_2} = 4.3702E - 6 \frac{X_{Pu,N}}{x_2}$$
 (51)

If N is a point along Cd/U phase boundary, then $x_2 = X_{Pu}^*$ and $y_1 = X_{U,N}$. Then, Equations 50 and 51 are simplified as below.

$$a_{U,N} = \frac{X_{U,N}}{y_1} = \frac{y_1}{y_1} = 1 \tag{52}$$

$$a_{Pu,N} = 4.3702E - 6\frac{X_{Pu,N}}{x_2} = 4.3702E - 6\frac{X_{Pu,N}}{X_{Pu}^*} = \gamma_{Pu}^* X_{Pu,N}$$
 (53)

If N is a point along the Cd/PuCd₆ phase boundary, then $y_1 = X_U^*$ and $X_{Pu,N} = x_2$. Then, Equations 50 and 51 are simplified as below.

$$a_{U,N} = \frac{X_{U,N}}{y_1} = \frac{X_{U,N}}{X_U^*} = \gamma_U^* X_{U,N}$$
 (54)

$$a_{Pu,N} = 4.3702E - 6\frac{X_{Pu,N}}{x_2} = 4.3702E - 6\frac{x_2}{x_2} = 4.3702E - 6$$
 (55)

Thus, the undersaturated domain model is consistent with the phase boundary model, with respect to the isoactivity of uranium and isoactivity coefficient of plutonium along the Cd/U phase boundary and the isoactivity of plutonium and isoactivity coefficient of uranium along the Cd/PuCd₆ phase boundary. Adapting Equation 11 to represent point N gives the following.

$$\frac{X_{PuCl_3,N}}{X_{UCl_3,N}} = k \frac{\gamma_{Pu,N} X_{Pu,N}}{\gamma_{U,N} X_{U,N}} \tag{56}$$

Equation 52 is combined with Equations 50 and 51 to give an expression for the Pu:U ratio in the salt at equilibrium with any point N.

$$\frac{X_{PuCl_3,N}}{X_{UCl_3,N}} = 4.3702E - 6\frac{y_1}{x_2}k\frac{X_{Pu,N}}{X_{U,N}}$$
(57)

Rearranging Equation 57 gives an expression for the separation factor at any point N.

$$SF_N = \frac{X_{PuCl_3,N}X_{U,N}}{X_{UCl_3,N}X_{Pu,N}} = 4.3702E - 6\frac{y_1}{x_2}k$$
 (58)

A contour surface of Pu:U ratios in the salt is superimposed above the cadmium phase field in Figure 7. The Pu:U ratios are presented in log scale. Similarly, a contour surface of separation factors is superimposed above the cadmium phase field in Figure 8.

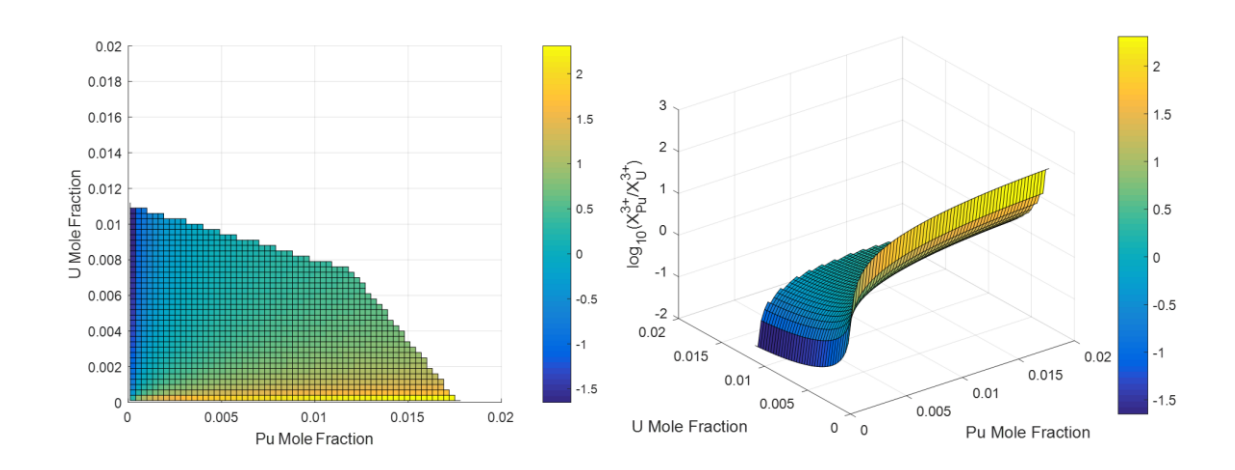


Figure 7. Contour Surface of Pu:U Ratio in the Salt

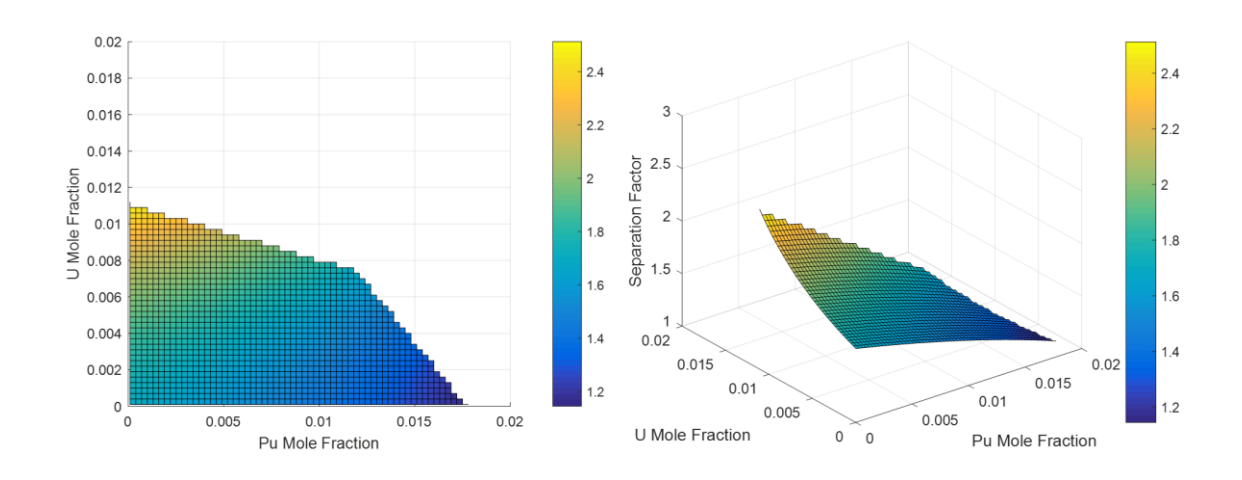


Figure 8. Contour Surface of Separation Factor

The plan views from Figures 7 and 8 are shown in Figure 9 with contour lines superimposed above the cadmium phase field. The contour lines represent the Pu:U ratios in the salt (left) and separation factors (right). The Pu:U ratios are presented in log scale. Like a topographical map, each contour line represents an iso-value.

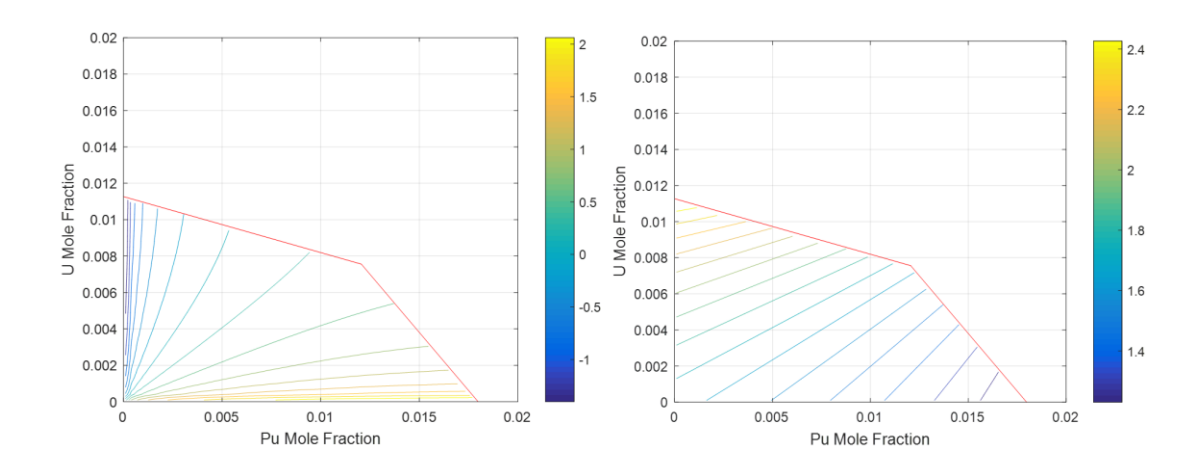


Figure 9. Contour Lines of Pu:U Ratio in the Salt (left) and Separation Factor (right)

Recovery of a U-Pu alloy for subsequent fuel fabrication is one practical aspect of using the cadmium system to extract uranium and plutonium from a molten salt. After extraction, the cadmium and salt are distilled away from the recovered product leaving behind a U-Pu alloy ingot.

A plan view of the cadmium phase field is shown in Figure 10 (left) with six contour lines representing unique U:Pu ratios of dissolved uranium and plutonium in the cadmium. The highest ratio is U:Pu = 4:1, and the lowest ratio is U:Pu = 1:8. The corresponding Pu:U ratio in the salt along each of these six lines is also shown in Figure 10 (right). This relationship is a direct illustration of how the Pu:U ratio in the salt determines U:Pu ratio in the recovered alloy product.

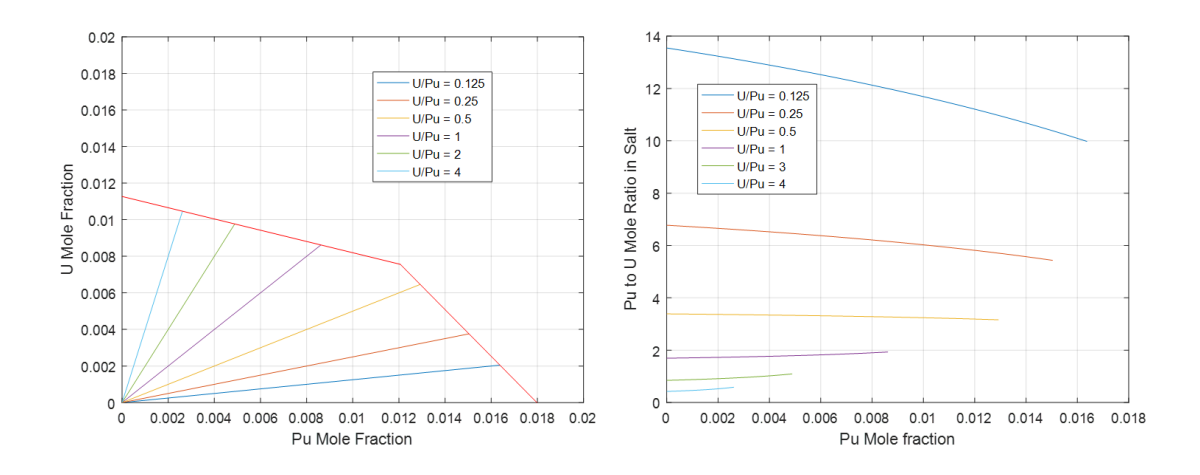


Figure 10. U:Pu Ratio Lines in the Cadmium (left) and Corresponding Pu:U Ratio Lines in the Salt (right)

The equation used to relate the Pu:U ratio in the salt to the U:Pu ratio in the product is a modification of Equation 57.

$$\frac{X_{PuCl_3}}{X_{UCl_3}} = 4.3702E - 6\frac{y_1}{x_2}k\frac{1}{(U:Pu)}$$
(59)

6. Model Validation

Experimental data representative of undersaturated equilibrium conditions within the cadmium phase are summarized in Table 3. Experimental data representative of saturation equilibrium conditions within the cadmium phase are summarized in Tables 4 and 5. The shaded row in Table 4 highlights data that may not represent equilibrium conditions.

Table 3. Analysis of Experimental Data at Undersaturation Conditions [10]

Experiment	Measured Pu (mole %)	Measured U (mole %)	Measured Pu:U Salt	Measured SF	Modeled Pu:U Salt	Modeled SF
2-1	0.4160	0.5547	1.45	1.93	1.39	1.85
2-1	0.3826	0.4925	145	1.86	1.42	1.82
2-1	0.1243	0.1578	1.45	1.84	1.36	1.73
2-1	0.0526	0.0669	1.45	1.84	1.34	1.71
2-2	0.4160	0.6503	1.36	2.13	1.22	1.91
3	0.6838	0.9229	1.47	1.99	1.53	2.06
3	0.6742	0.8990	1.47	1.96	1.53	2.06
3	0.4543	0.5690	1.47	1.85	1.48	1.85
3	0.3634	0.4447	1.47	1.80	1.47	1.80
3	0.2616	0.2831	1.47	1.59	1.61	1.75
4	0.4065	0.7316	1.13	2.04	1.10	1.98
4	0.2104	0.3634	1.13	1.96	1.04	1.80
5-1	0.3586	0.5834	1.16	1.88	1.16	1.89
5-1	0.2821	0.4591	1.16	1.88	1.13	1.83
5-1	0.1769	0.2869	1.16	1.87	1.09	1.77
5-2	0.3586	0.5834	1.14	1.86	1.16	1.89
5-2	0.2821	0.4591	1.14	1.86	1.13	1.83
5-2	0.1913	0.3013	1.14	1.80	1.13	1.77
5-3	0.3156	0.5164	1.13	1.84	1.13	1.86
5-3	0.2487	0.3921	1.13	1.78	1.14	1.80
5-3	0.1482	0.2295	1.13	1.74	1.13	1.75
5-4	0.3108	0.5069	1.11	1.81	1.14	1.85
5-4	0.2248	0.3634	1.11	1.80	1.11	1.80
5-4	0.1339	0.2056	1.11	1.71	1.14	1.74

Table 4. Analysis of Experimental Data at Saturation Conditions [10]

Experiment	Measured Pu (mole %)	Measured U (mole %)	Measured Pu:U Salt	Measured SF	Modeled Pu:U Salt	Modeled SF
DE 1-2	0.507	1.019	1.454	2.94	1.111	2.23
DE 2-2	0.631	1.033	1.364	2.23	1.349	2.21
DE 4	0.550	1.057	1.132	2.18	1.180	2.27
EE 3	0.708	0.956	1.473	1.99	1.545	2.09
EE 5-1	0.545	0.928	1.156	1.96	1.242	2.11
EE 5-2	0.564	0.956	1.143	1.94	1.262	2.14
EE 5-3	0.531	0.913	1.127	1.94	1.223	2.10
EE 5-4	0.536	0.928	1.112	1.92	1.223	2.12

Table 5. Experimental Data at Saturation Conditions [9]

Measured Pu (mole %)	Measured U (mole %)
1.8171	0
1.5780	0.2774
1.4824	0.3969
1.4824	0.3491
1.3389	0.6121
1.2911	0.5786
1.0520	0.8655

The compositions of the data in Tables 3, 4, and 5 are shown on the cadmium phase field in Figure 11 along with the contour lines of the modeled separation factors first shown in Figure 9. The saturation data in Tables 4 and 5 were used earlier in Figure 4 in connection with the strategy used to determine the locations of the Cd/U and Cd/PuCd₆ phase boundaries.

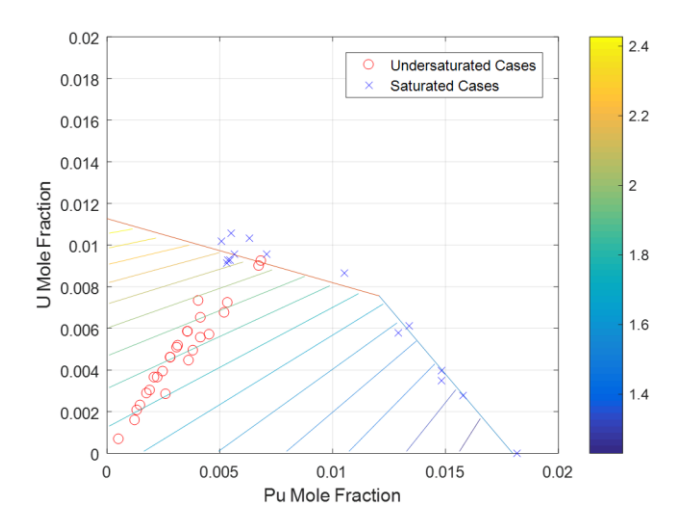


Figure 11. Contour Lines of Separation Factor

The measurement of separation factor involves sampling and analytical errors. In this example, it requires sampling the salt and cadmium, and analyzing each sample for uranium and plutonium. Therefore, if the standard error of each of the four analyses is approximately 5%, then the standard error of the resulting measured separation factor is approximately 10%. The measured and modeled separations factors from the data sets in Tables 3 and 4 are compared in Figure 12. The error bars represent 10% standard error. Nearly every error bar encloses the corresponding modeled value; and those few that do not would if the standard error was only slightly greater.

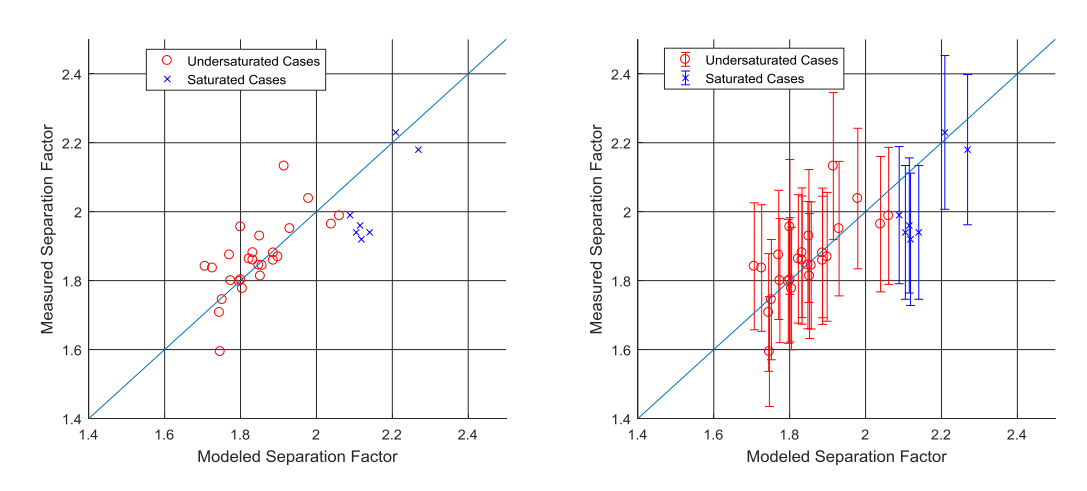


Figure 12. Comparison of Measured and Modeled Separations Factors

7. Predicted Separation Behavior of Lanthanides

In practice, the goal of exploiting the properties of cadmium is to achieve a low separation between plutonium and uranium (as a means of retaining plutonium and uranium as a group in the fuel cycle) and a high separation between plutonium and lanthanide (as a means of rejecting lanthanides from the fuel cycle). Equations 8, 11, and 12 are recast here in terms of plutonium and a lanthanide (Ln). Major lanthanide fission products include cerium, neodymium, samarium, and gadolinium.

$$PuCl_3(salt) + Ln(cadmium) = LnCl_3(salt) + Pu(cadmium)$$
 (60)

$$\frac{\gamma_{Ln}X_{Ln}}{\gamma_{Pu}X_{Pu}} = k\frac{X_{LnCl_3}}{X_{PuCl_3}} \tag{61}$$

$$k = exp\left(\frac{\Delta G_{f,LnCl_3}^0 - \Delta G_{f,PuCl_3}^0}{RT}\right) \frac{\gamma_{LnCl_3}}{\gamma_{PuCl_3}}$$
(62)

Equation 44 is recast in terms of the separation factor for plutonium relative to lanthanide and combined with Equation 61.

$$SF = \frac{(X_{PuCl_3}: X_{LnCl_3})_{Salt}}{(X_{Pu}: X_{Ln})_{Cadmium}} = \frac{X_{PuCl_3}X_{Ln}}{X_{LnCl_3}X_{Pu}} = k\frac{\gamma_{Pu}}{\gamma_{Ln}}$$
(63)

With Equation 63, the separation factor decreases as the stability of the lanthanide in the salt increases (based on the lower standard state Gibbs free energy of formation of its metal chloride). On the other hand, the separation factor increases as the stability of the lanthanide in the cadmium increases (based on

the lower activity coefficient of its dissolved metal in cadmium). These two factors work in tandem to determine the separation factor for various lanthanides against the reference species, plutonium.

The solution strategy developed in the previous sections was used to predict the behavior of plutonium and cerium in a salt/cadmium system at 500°C. The thermodynamic data from the literature for the salt system are given in Table 6 (analogous to Table 1). The thermodynamic data from the literature and the thermodynamic data predicted by the solution strategy are given in Table 7 (analogous to Table 2). The concentration of plutonium in the cadmium at the inflection point was kept the same as before in Equation 41. In the absence of experimental data to support the location of the phase boundaries, this was a reasonable approximation. Experimentally derived phase diagrams for the Cd-Ce [12, 15] binary alloy system show that cerium saturated cadmium is in equilibrium with the cerium-cadmium intermetallic CeCd₁₁.

Table 6. Thermodynamic Values for the PuCl₃ and CeCl₃ Salt System

Parameter	Value	Reference
$\Delta G_{f,CeCl_3}^0$ at 500°C	-854.297 kJ mol ⁻¹	[6]
$\Delta G_{f,PuCl_3}^0$ at 500°C	-771.377 kJ mol ⁻¹	[6]
γ_{CeCl_3}	0.0118	[12]
γ_{PuCl_3}	0.00662	[7]
R	8.31451 J K ⁻¹ mol ⁻¹	[8]
T	773.15 K	
k	6.182E5	

Table 7. Thermodynamic Values for the Cd-Pu-Ce Alloy System

Parameter	Value
Saturation limit of Ce in Cd-Ce binary alloy.	0.006012 mole fraction [13]
Activity coefficient of Ce in Cd-Ce binary alloy.	1.4704E-8
Saturation limit of Pu in Cd-Pu binary alloy.	0.01798 mole fraction
Activity coefficient of Pu in Cd-Pu binary alloy.	2.4310E-4
Equation describing the Cd/CeCd ₁₁ phase boundary.	$X_{Ce,1} = -0.1641 X_{Pu,1} + 0.0066,$ or $X_{Pu,1} = -6.0925 X_{Ce,1} + 0.0366$
Equation describing the Cd/PuCd ₆ phase boundary	$X_{Ce,2} = -0.6812 X_{Pu,2} + 0.0122,$ or $X_{Pu,2} = -1.4681 X_{Ce,2} + 0.0180$
Location of Inflection Point	$X_{Ce}^* = 0.004033$ $X_{Pu}^* = 0.01206$
Activity of Ce along the Cd/CeCd ₁₁ phase boundary.	8.840E-11 [14]
Activity coefficient of Ce along the Cd/PuCd ₆ phase boundary.	2.192E-8
Activity of Pu along the Cd/PuCd ₆ phase boundary.	4.370E-6
Activity coefficient of Pu along the Cd/CeCd ₁₁ phase boundary.	3.624E-4

The separation factor as a function of the Pu:Ce ratio in the salt, for conditions unique to the $Cd/CeCd_{11}$ and $Cd/PuCd_6$ phase boundaries is shown in Figure 13 (analogous to Figure 5). The upper and lower separation factor limits are 0.0346 and 0.0156, respectively. The separation factor at the inflection point is 0.0232.

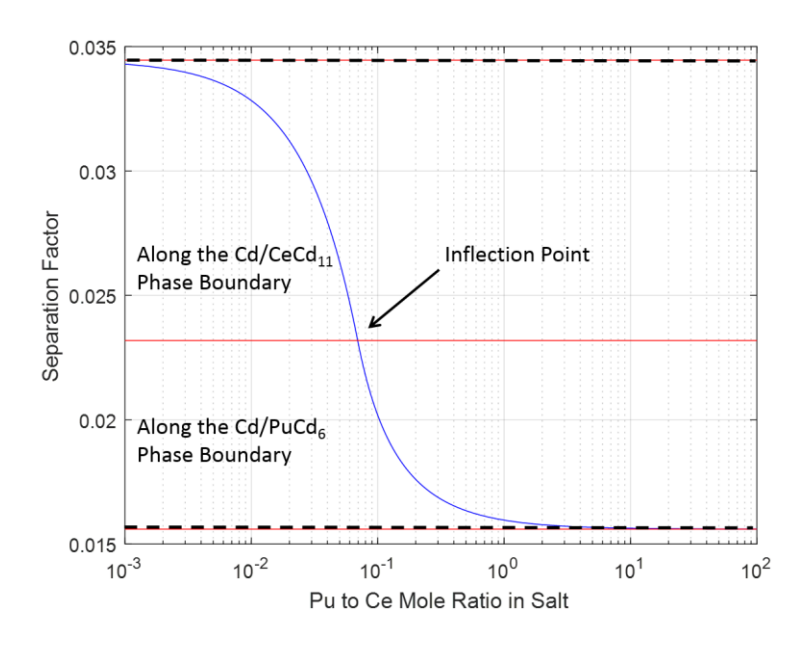


Figure 13. Conditions along the Phase Boundaries

A contour surface of Pu:Ce ratios in the salt is superimposed above the cadmium phase field in Figure 14 (analogous to Figure 7). The Pu:Ce ratios are presented in log scale. Similarly, a contour surface of separation factors is superimposed above the cadmium phase field in Figure 15 (analogous to Figure 8).

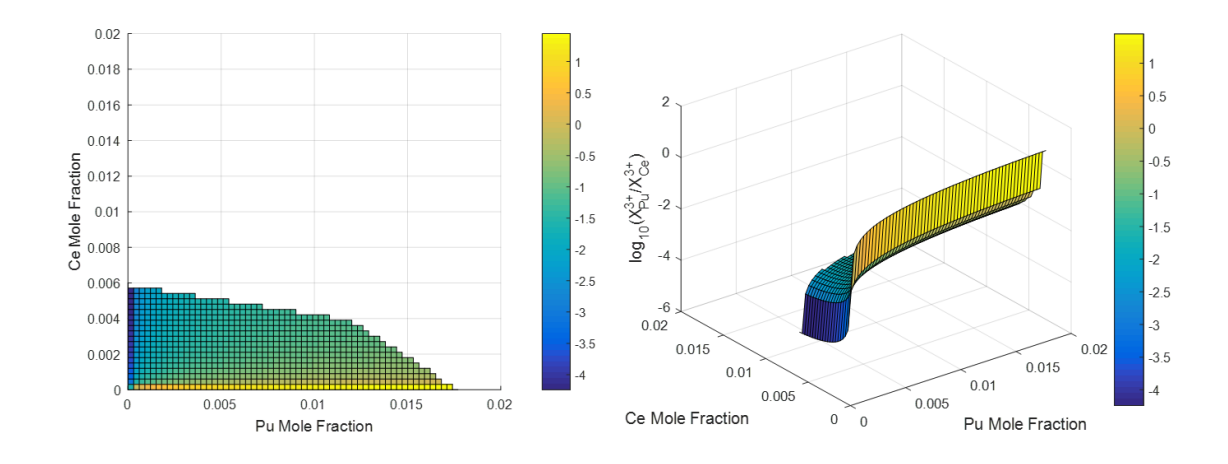


Figure 14. Contour Surface of Pu:Ce Ratio in the Salt

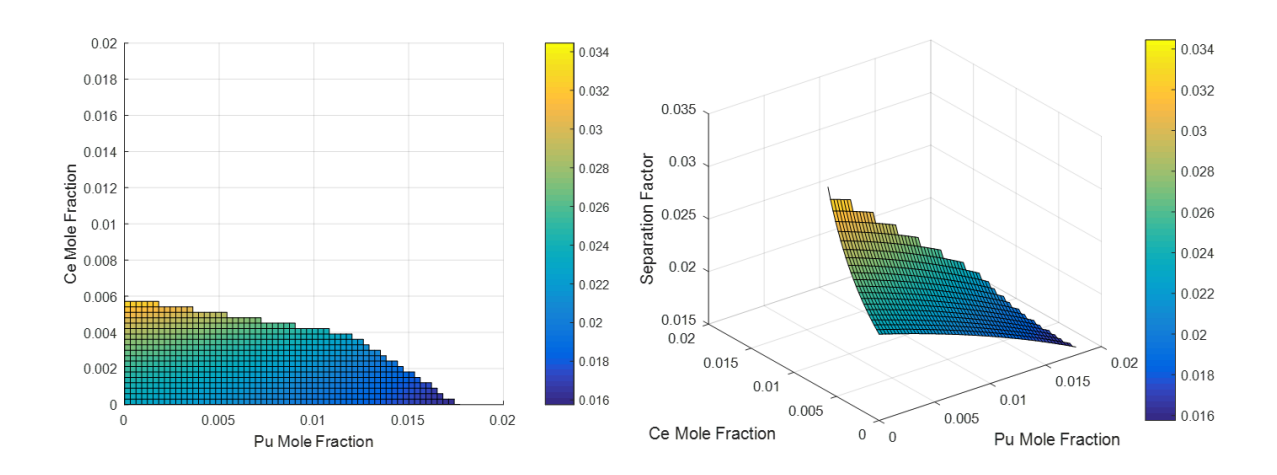


Figure 15. Contour Surface of Separation Factor

The plan views from Figure 14 and 15 are shown in Figure 16 (analogous to Figure 9) with contour lines superimposed above the cadmium phase field. The contour lines represent the Pu:Ce ratios in the salt (left) and separations factors (right). The Pu:Ce ratios are presented in log scale.

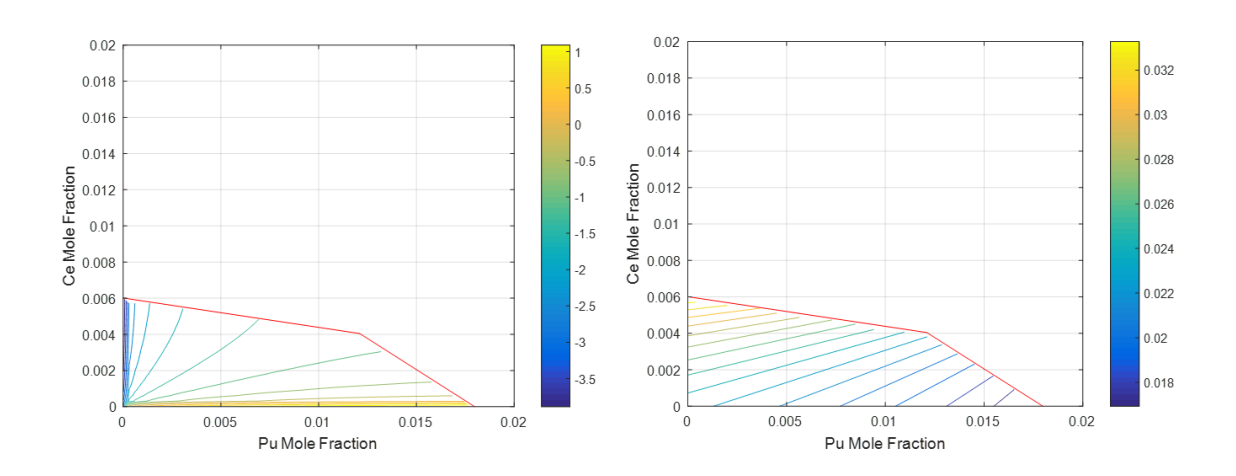


Figure 16. Contour Lines of Pu:Ce Ratio in the Salt (left) and Separation Factor (right)

8. Discussion and Conclusions

Liquid cadmium "extraction" systems are configured in different ways; a few examples are given below. Charge neutrality of the salt is always maintained. In the absence of a chlorine evolving anode, cations reduced at the cadmium interface must be replaced by other cations oxidizing into the salt. For example, if a uranium anode is connected to a cadmium cathode, the uranium and plutonium cations reduced into the cathode are replaced only by uranium cations oxidized at the anode. Therefore, as uranium and plutonium reduction proceeds at the cadmium interface, the concentration of UCl₃ increases, while the concentration of PuCl₃ decreases, but the sum of the concentrations of UCl₃ and PuCl₃ remains constant.

• Galvanic. Current between the anode and cathode is driven by the resulting potential difference. Metal (ME) electrode assemblies provide a junction.

$$Common|ME|Uranium||Salt||Cadmium|ME|Common$$
 (64)

• Electrolytic. Current between the anode and cathode is driven by an external power supply. Metal (ME) electrode assemblies provide a junction.

$$(+)|ME|Uranium||Salt||Cadmium|ME|(-)$$
(65)

Chemical. Current across the salt/cadmium interface is driven by a reactive metal in the cadmium.

$$Salt || Cadmium || Uranium$$
 (66)

In any case, the further the system is driven from equilibrium conditions, the more influential are the kinetic effects. However, if the ending condition of the galvanic, electrolytic, or chemical "extraction" system is one of equilibration with the salt, then the interpretation presented here applies.

In a LiCl-KCl eutectic salt with solute concentrations of UCl₃ and PuCl₃, the reduction potentials of uranium and plutonium are approximately -1.3 V and -1.7 V, respectively, as pure metal deposits, relative to the Ag/AgCl reference electrode [11], at 500°C. This 400 mV difference allows successful electrorefining of high-purity uranium in the presence of PuCl₃. And for codeposition of uranium and plutonium to occur, it is first necessary to overcome the limiting current of uranium reduction in order drive the cathode to the more negative reduction potential of plutonium. However, when cadmium is introduced, uranium and plutonium are reduced at the same potential as described here. Such constraints explain why it is impossible under any conditions to reduce plutonium and uranium from the salt at a Pu:U ratio greater than that of the salt. In other words, the separation factor as defined here must always be greater than one.

Separation factor was defined in Equation 44 as the ratio of two ratios; the Pu:U ratio in the salt divided by the Pu:U ratio in the cadmium. Here "in the cadmium" means the undersaturated cadmium up to the saturation limits that were defined by the Cd/U and Cd/PuCd₆ phase boundaries. Within these boundaries the cadmium is a single phase with dissolved uranium and plutonium. Beyond these boundaries other solid phases are introduced, either uranium metal or PuCd₆ intermetallic, that are in equilibrium with the cadmium, while existing as a separate phase from the cadmium. Therefore, a separation factor that considers only the cadmium phase is quite different from a separation factor that considers the cadmium phase, uranium phase, and PuCd₆ phase combined. This latter separation factor has value only as an empirical measure of the separation performance of a particular experimental result.

Separation factors are a useful measure of separation performance, which is determined by the underlying thermodynamic and kinetic factors that dictate the extent to which species partitioning between phases. The thermodynamic derivation presented here clearly illustrates the dynamic nature of separation factor as a response to separation performance. Furthermore, there is significant error associated with both the theoretical calculation, and the experimental measurement, of separations factors.

The equilibrium interaction between the liquid cadmium phase field of the Cd-U-Pu ternary alloy system, and molten salt containing solute concentrations of UCl₃ and PuCl₃ is modeled using a combination of experimental data, thermodynamic relationships, and a geometric interpretation of the cadmium phase field. The model is such that continuity is maintained of thermodynamic functions and phase relations.

The Pu:U ratio in the salt at the inflection point was given in Equation 28. The implication is that when the Pu:U ratio in the salt is less than 2.7, further deposition of metal (uranium or plutonium) into the cadmium phase will result in the formation of a uranium metal phase. And when the Pu:U ratio in the salt is greater than 2.7, further deposition of metal (uranium or plutonium) into the cadmium phase will result

in the formation of a PuCd₆ intermetallic phase. These statements are correct only if, after the deposition of metal, the salt and cadmium phases return to equilibrium and the assumed phase field in Figure 2 is correct.

9. Acknowledgements

The effort to prepare this manuscript was supported by the U.S. Department of Energy Nuclear Technology Research & Development Program. The manuscript is based on a series of technical internal memorandum prepared by the authors in 2009.

10. References

- 1. Irving Johnson and Harold M. Feder, "Thermodynamics of the Uranium-Cadmium System", Transactions of the Metallurgical Society of AIME, Vol. 224, pp. 468-473, 1962
- 2. Allan E. Martin, Irving Johnson, and Harold M. Feder, "The Cadmium-Uranium Phase Diagram", Transactions of the Metallurgical Society of AIME, Vol. 221, pp. 789-791, August, 1961
- 3. Irving Johnson, Martin G. Chasanov, and Robert M. Yonco, "Pu-Cd System: Thermodynamic and Partial Phase Diagrams", Transactions of the Metallurgical Society of AIME, Vol. 233, pp. 1408-1414, July, 1965
- 4. F. H. Ellinger, R. O. Elliott, and E. M. Cramer, "The Plutonium Uranium System", Journal of Nuclear Materials, Vol. 3, pp. 233-243, 1959
- 5. SigmaStat Version 3.5 software
- 6. HSC Chemistry, Version 8.1.1 software, Outotec
- 7. T. Koyama, T. R. Johnson, and D. F. Fisher, "Distribution of Actinides in Molten Chloride Salt/Cadmium Metal Systems", Journal of Alloys and Compounds, Vol. 189, pp. 37-44, 1992
- 8. "IUPAC Quantities, Units, and Symbols in Physical Chemistry, 2nd Edition", Blackwell Scientific Publications, ISBN 0-632-03583-8, 1993
- 9. Koichi Uozumi, Masatoshi Iizuka, Tetsuya Kato, Tadashi Inoue, Osamu Shirai, Takashi Iwai, and Yasuo Arai, "Electrochemical Behaviors of Uranium and Plutonium at Simultaneous Recoveries into Liquid Cadmium Cathodes", Journal of Nuclear Materials, Vol. 325, pp. 34-43, 2004
- Yoshiharu Sakamura, Masatoshi Iizuka, Tadafumi Koyama, Sinichi Kitawaki, and Akira Nakayoshi, "Novel Approach to Extracting Transuranic Elements in Molten Salt Electrorefining", Nuclear Technology, Vol. 190, pp. 193-206, 2015
- 11. L. Yang and R. G. Hudson, "Some Investigations of the Ag-AgCl in LiCl-KCl Eutectic Reference Electrode", Journal of the Electrochemistry Society, Vol. 106, pp. 986-9960, 1959
- 12. K. C. Marsden and B. Pesic, "Evaluation of the Electrochemical Behavior of CeCl₃ in Molten LiCl-KCl Eutectic Utilizing Metallic Ce as an Anode", Journal of the Electrochemical Society, Vol. 158, pp. F111-F120, 2011
- 13. Irving Johnson, Karl E. Anderson, and Robert A. Bloomquist, "Partial Constitutional Diagrams for the Cd-La, Cd-Ce, Cd-Pr, Cd-Nd, and Cd-Sm Systems", Transactions of the ASM, Vol 59, pp.352-355, 1966
- 14. Si-Hyung Kim, Seungwoo Peak, Tack-Jin Kim, Dae-Yeob Park, and Do-Hee Ahn, "Electrode Reactions of Ce³⁺/Ce Couple in LiCl-KCl Solutions Containing CeCl₃ at Solid W and Liquid Cd Electrodes", Electrochimica Acta, Vol. 85, pp. 332-335, 2012
- 15. Irving Johnson and Robert M. Yonco, "Thermodynamics of Cadmium- and Zinc-Rich Alloys in the Cd-La, Cd-Ce, Cd-Pr, Zn-La, Zn-Ce and Zn-Pr Systems", Metallurgical Transactions, Vol. 1, pp. 905-910, 1970 (Correction Issued, Vol. 1, pp. 2330, 1970)